OXIDATIVE STRESS AS A MEDIATOR OF THE IMMUNOMODULATION EXERTED BY MONOCLONAL ANTIBODIES IN THE TREATMENT OF LUNG CANCER IN MICE

Jun Tang, Daniel Ramis-Cabrer, Xuejie Wang, and Esther Barreiro

[1]Pulmonology Department-Muscle and Respiratory System Research Unit (URMAR), IMIM-*Hospital del Mar*, *Parc de Salut Mar*, Health and Experimental Sciences Department (CEXS), *Pompeu Fabra* University (UPF), Department of Medicine, Autonomous University of Barcelona (UAB), Biomedical Research Park (PRBB), C/ Dr. Aiguader, 88, Barcelona, E-08003 Spain.

[2]*Centro de Investigación en Red de Enfermedades Respiratorias* (CIBERES), *Instituto de Salud Carlos* III (ISCIII), C/ Monforte de Lemos 5, Madrid, E-28029 Spain.

Corresponding author: Dr. Esther Barreiro, Pulmonology Department-URMAR, IMIM-Hospital del Mar, PRBB, C/ Dr. Aiguader, 88, Barcelona, E-08003 Spain, Telephone: (+34) 93 316 0385, Fax: (+34) 93 316 0410, e-mail: ebarreiro@imim.es.

Short title: Immunomodulators in therapy of lung adenocarcinoma

Word count: 3,943

ABSTRACT

Background: Lung cancer (LC) is a major leading cause of death worldwide. Immunomodulators that target several immune mechanisms have proven to reduce tumor burden in experimental models through induction of the immune microenvironment. We hypothesized that other biological mechanisms may also favor tumor burden reduction in lung cancer-bearing mice treated with immunomodulators. **Methods:** Tumor weight, area, and immune cells (T, B, macrophages, and TNF-alpha levels, immunohistochemistry) and tumor growth, oxidative stress, apoptosis, autophagy, and sirtuin-1 markers were analyzed (immunoblotting) in subcutaneous tumor of BALB/c mice injected with LP07 adenocarcinoma cells treated with monoclonal antibodies (CD-137, CTLA-4, PD-1, and CD-19, N=9/group) and non-treated control animals. **Results:** Compared to non-treated cancer mice, in tumors of monoclonal-treated animals, tumor area and weight and ki-67 significantly reduced, while T cell counts, oxidative stress, apoptosis, autophagy, and sirtuin-1 marker increased. **Conclusion:** **I**mmunomodulators elicited a reduction in tumor burden (reduced tumor size and weight) through decreased tumor proliferation and increased oxidative stress, apoptosis, autophagy, and sirtuin-1 levels, which may have interfered with the immune profile of the tumor microenvironment. Future research should be devoted to the elucidation of the specific contribution of each biological mechanism to the reduced tumor burden.

Word count: 194

KEY WORDS: experimental lung cancer; immunomodulators; oxidative stress; autophagy; tumor growth; sirtuin-1

INTRODUCTION

Lung cancer is the most prevalent cancer worldwide that affects both sexes and has a very high mortality [1]. Despite the development of new therapeutic strategies, patients with lung cancer have an overall survival rate lower than 15% in five years [1-3]. Respiratory conditions such as chronic obstructive pulmonary disease (COPD) and lung fibrosis predispose patients to a greater risk to develop lung cancer, especially non-small cell lung cancer (NSCLC) type [1;2;4-6].

The underlying biology of lung cancer is complex as several mechanisms may interplay at different stages. For instance, inflammation, which is key in host protection, may promote lung cancer initiation and malignancy in chronic inflammatory processes such as in patients with COPD [2;5;7-11]. Moreover, oxidative stress was also shown to participate in tumor initiation, promotion and progression of carcinogenesis in patients with lung cancer particularly in those with COPD [2;9;12;13]. Besides, inflammatory events and oxidative stress may drive the release of a cascade of cytokines and growth factors, which may favor lung tumorigenesis [2;9;12;13] through interference with biological processes such as apoptosis and autophagy [11;13-15]. In the last few years, the implications of biological mechanisms such as increased oxidative stress, inflammatory events, particularly a Th1 predominant response, and epigenetic events were demonstrated to be differentially expressed in the lung tumors of patients with COPD compared to patients without this respiratory condition [8;11;13;16]. These results are important, since they may help establish a differential profile of patients that may be more or less susceptible to certain therapies.

The immune system defends host against diseases including neoplastic transformation. However, cancer cells may evade the host immune system through a process defined as cancer immunoediting [17]. Cancer immune scape results from the action of immunosuppressive pathways that involve membrane receptors that are located in immune cell types along different steps of the cancer-immunity cycle [17-21]. Immune checkpoints enable immune tolerance to

prevent autoimmunity events in the host [17-22]. Several immune checkpoints have been identified so far. As such, programmed cell death protein 1 (PD1) is a membrane receptor that promotes immune tolerance through T cell inactivation [18;19;22]. Cytotoxic T-lymphocyte associated protein 4 (CTLA-4) is a disruptor of antigen presentation upon T cell activation [17]. Cluster of differentiation 137 (CD137) is located in several immune cells such as T regulatory cells (Treg) that are responsible for repressing T cell activity [21]. Additionally, B cells present cluster of differentiation 19 (CD19), which can trigger pro- and anti-tumorigenic responses [20].

Specific immune checkpoint inhibitors have been designed, namely monoclonal antibodies that specifically act against these membrane receptors in order to boost the immune microenvironment. The blockade of these inhibitory pathways has been shown to restore the anti-tumor activity of the immune system [17;22-25]. The therapeutic efficacy of the combination of different immunomodulatory monoclonal antibodies has been recently demonstrated in animal models of lung cancer, in which the tumor immune microenvironment was specifically explored [18;19]. Furthermore, in previous studies from our group [8;11-13;16;26], the contribution of inflammation, oxidative stress, autophagy, and apoptosis in response to several pharmacological strategies was shown in mice bearing lung tumors. Whether similar biological mechanisms can be observed in the tumors of mice treated with a combination of several immunomodulators remains to be identified. Thus, we reasoned that immunomodulators may also exert beneficial effects on tumor burden through biological events other than the immune microenvironment.

On this basis, we hypothesized that treatment of a combination of specific immunomodulatory monoclonal antibodies that included anti-PD1, anti-CTLA-4, anti-CD137, and anti-CD19 may have an effect on tumor progression through several biological mechanisms such as oxidative stress, autophagy, and apoptosis in wild type lung adenocarcinoma cells of mice [26]. Accordingly, in the current investigation, the main objectives were two-fold: 1) to

assess the immune tumor microenvironment (T and B cells, macrophages, and inflammatory cytokines) and 2) to quantify levels of oxidative stress, antioxidant enzymes, apoptosis, autophagy, and cell proliferation rates in the subcutaneous lung adenocarcinoma tumors of BALB/c mice treated with a combination of immunomodulators (anti-PD1, anti-CTLA-4, anti-CD137, and anti-CD19 monoclonal antibodies). A group of tumor-bearing mice that did not receive treatment with the cocktail of monoclonal antibodies was the control group in the study. This experimental model of NSCLC has been well-validated in our group [12;26-29].

METHODS

Animal experiments

Experimental design. The study protocol is illustrated in Figure 1. An animal model with lung cancer was developed through the inoculation of cancer cells from LP07 stable adenocarcinoma cell line derived from P07 lung tumor that spontaneously appeared in BALB/c mice [30-32]. Eighteen female BALB/c mice (8 weeks old, 20 g weight) acquired from *Harlan Interfauna Ibérica SL* (Barcelona, Spain) received a subcutaneous inoculation of LP07 cells (4×10^5) resuspended in 0.2 mL of minimal essential medium (MEM) in the left flank (Figure 1). After tumor cell inoculation on day 0 of all the mice, they were randomly divided into two independent groups (N=9/group) to be thereafter followed for 30 days: 1) experimental control group in which mice received an intraperitoneal administration of 0.2 mL phosphate-buffered saline (PBS) every 72 hours (non-treated controls group) and 2) mice treated with a combination of monoclonal antibodies (treated lung cancer group) that included anti-PD1 (RMP1-14; Cat. #BE0146, BioXCell, Nuevo Hampshire, USA), anti-CTLA-4 (9D9; Cat. #BE0164, BioXCell), anti-CD137 (LOB12.3; Cat. #BE0169, BioXCell) and anti-CD19 (1D3; Cat. #BE0150, BioXCell) antibodies [21;33-36]. A dose of 5×10^{-3} mg/kg/72h in 0.2 mL PBS was administered to the treated group of lung cancer mice from day 15 (tumors visible) up until day 30 (Figure 1). For ethical reasons we were not allowed to extend the study protocol longer than 30 days.

Peer-reviewed version available at Cancers 2019, 11, 1301; doi:10.3390/cancers11091301

Food and water were supplied *ad libitum* and mice were kept under pathogen-free conditions with a 12: 12 h light: dark cycle in the animal facilities placed in the *Barcelona Biomedical Research Park* (PRBB) premises.

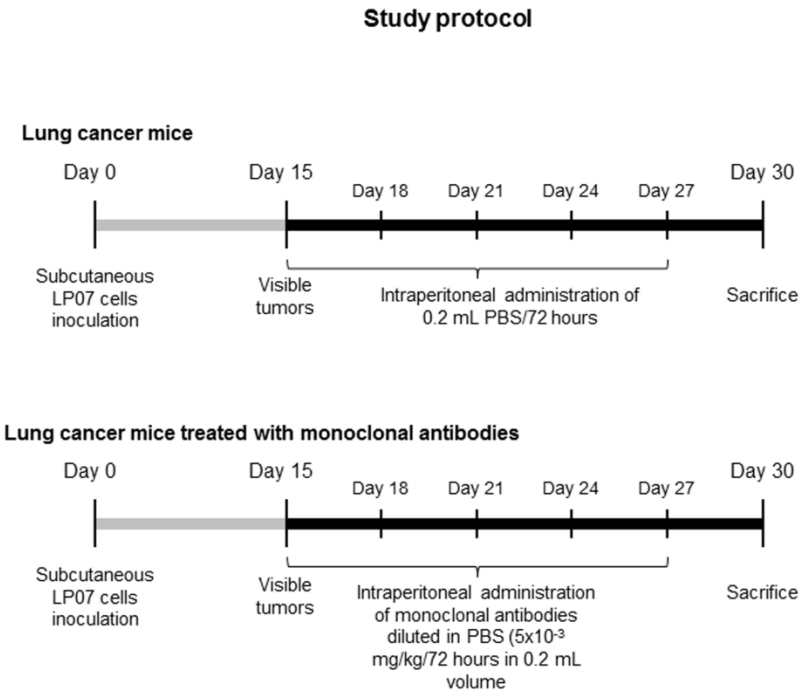

Figure 1: Graphical time-line representation of the non-treated control lung cancer mice and the lung cancer group of animals treated with the combination of monoclonal antibodies.

This was a controlled study designed according to the ethical regulations on animal experimentation of the Spanish Legislation (Real Decreto 53/2013, BOE 34/11370–11421), the European Community Directive 2010/63/EU, and the European Convention for the Protection of Vertebrate Animals Used for Experimental and Other Scientific Purposes (1986) at PRBB. Animal Research Committee approved all animal experiments (Animal Welfare Department in Catalonia, Spain, # EBP-15-1704).

In vivo measurements conducted on the animals. Food intake and body weight were measured daily in all the study animals. Tumor area was also measured daily using a specific caliper in all the animals.

Sacrifice and sample collection. The two experimental groups of mice were sacrificed after 30 days of inoculation of LP07 cells. In each mouse an intraperitoneal injection of 0.1 ml sodium

pentobarbital (60 mg/kg) was inoculated to anesthetize. In order to verify total anesthesia depth, the pedal and blink reflexes were assessed in all animals. The subcutaneous tumor was extracted from all the mice. A fragment of the tumor specimens was immediately frozen in liquid nitrogen and stored at -80ºC, while the other fragment was immersed in an alcohol-formol to be thereafter embedded in paraffin until further use.

Molecular biology analyses

Histological analyses of tumor samples. Immunohistochemical techniques were applied on tumor sections in order to explore expression of the proliferation marker Ki-67, T and B cells, macrophages, and the inflammatory cytokine tumor necrosis factor (TNF)-alpha following previous methodologies [8;12;13;16;26-29;37;38]. Briefly, for all the target antigens, tumor cross-sections were deparaffinized and then antigen retrieval was carried out by heating slides in a water bath in Tris/Ethylenediaminetetraacetic acid (EDTA) buffer pH 9 for 30 minutes (Ki-67, CD3, CD20, CD68, TNF-alpha) or in a pressure-cooker (CD4, CD8) in 0.1M citrate buffer pH 6 for 15 minutes. Subsequently, samples were blocked with 3% H_2O_2 for 15 minutes and immediately afterwards they were blocked with 1% BSA and goat serum for 2 hours. Slides were then incubated at room temperature for 30 minutes (CD3, CD68, TNF-alpha) or at 4ºC overnight (Ki-67, CD4, CD8, CD20) with the following specific primary antibodies: anti-Ki67 (Merck-Millipore, Darmstadt, Germany), anti-CD3 (DAKO, Glostrup, Denmark), anti-CD4 (Abcam, Cambridge, UK), anti-CD8 (Abcam) and anti-CD68 (Abcam), anti-CD20 (Invitrogen,Carlsbad, CA, USA), and anti-TNF-alpha (Santa Cruz, Santa Cruz, CA, USA). Slides were washed and incubated for 30 minutes with biotinylated universal secondary antibody followed by incubation for 30 minutes with horseradish-conjugated streptavidin and diaminobenzidine for 5 minutes (kit LSAB+HRP Dako Cytomation Inc., Carpinteria, CA, USA) as a substrate. Tumor sections were counterstained with hematoxylin for two minutes and were then dehydrated and mounted for conventional microscopy. Images of the stained tumors were taken under a light microscope (Olympus BX 61, Olympus Corporation, Tokyo,

Japan) coupled with a camera (Olympus DP 71, Olympus Corporation). Results are expressed as the percentage of stained nuclei for each of the tumors in the two groups of mice. The number of Ki-67, CD3, CD8, and CD68 cells was expressed as the percentage of the cells that were positively stained for the corresponding markers of the total cells in the tumor preparations. The number of CD4 cells was represented as the number of cells that were positively stained for CD4 in the measured area (expressed in micrometers). The numbers of CD20 and TNF-alpha cells were estimated using the semiquantitative immunohistochemical scoring system (HSCORE) according to methodologies previously published [39;40]. CD20 and TNF-alpha staining in the tumor preparations were classified according to the following categories: 0, 1, 2, 3, 4 and 0, 1, 2, 3 (0 indicates the absence of staining), respectively. The histochemical score (Hscore) for each tumor preparation was calculated as the percentage of tumor cells in each category (P) multiplied by the corresponding category: Hscore 1= P1 x 1; Hscore 2 =P2 x 2; Hscore 3=P3 x 3; and Hscore 4= P4 x 4, where Hscore 1 was the lowest positive and Hscore 4 was the highest positive level. In addition, Hscore 0 was established as the percentage of negatively stained cells for the corresponding antibodies.

Terminal deoxynucleotidyl transferase- mediated uridine 5'-triphosphate (UTP) nick- end labelling (TUNEL) assay. In tumor paraffin-embedded sections, apoptotic nuclei were identified using the TUNEL assay (In Situ Cell Death Detection Kit, POD, Roche Applied Science, Mannheim, Germany) of all study groups following the manufacturer's instructions and previous studies [29;38]. Briefly, this assay is based on the principal that during apoptotic nuclei genomic DNA may yield double-stranded, low molecular weight fragments as well as single strand breaks (nicks) in high molecular weight DNA. This DNA strand breaks can be identified by labelling 3'-hydroxyl (3'OH) groups with modified nucleotides in an enzymatic reaction. In this assay, deoxynucleotidyl transferase (TdT), which catalyzes the polymerization of nucleotides to free 3'-OH DNA ends, is used to label DNA strand breaks. Briefly, diaphragm and gastrocnemius muscle sections were fixed and permeabilized. Subsequently, they were

incubated with the TUNEL reaction mixture that contains terminal TdT and fluorescein-dUTP. During the incubation period, terminal TdT catalyzed the addition of fluorescein-dUTP at free 3'-OH groups in single- and double- stranded DNA. After washing, the label incorporated at the damaged sites of the DNA was marked by anti-fluorescein antibody conjugated with the reporter enzyme peroxidase. After several washes that removed unbound enzyme conjugate, the peroxidase retained in the immune complex was visualized by a substrate reaction. Apoptotic nuclei were brown, while negative nuclei were blue (hematoxylin counterstaining). In each tumor cross-section, the TUNEL-positive nuclei and the total number of nuclei were counted blindly by 2 independent observers, who were previously trained for that purpose. Results were expressed as the ratio of total TUNEL positively-stained nuclei to the total number of counted nuclei, as also previously reported [29;38]. A minimum amount of 300 nuclei were counted in each tumor preparation. Final results corresponded to the mean value of the counts provided by the 2 independent observers (concordance rate 95%). Negative control experiments, in which the TUNEL reaction mixture was omitted, were also conducted. Moreover, rat testicles were used as a positive control in these experiments.

Immunoblotting. Protein levels of the target markers were determined using 1D electrophoresis and immunoblotting according to previously published methodologies [8;12;13;16;26-29;37]. Frozen tumor samples extracted from mice were homogenized in lysis buffer. The following specific primary antibodies were used to identify the different target markers: protein tyrosine nitration (anti-3-nitrotyrosine antibody, Invitrogen, Eugene, Oregon, USA), malondialdehyde protein adducts (anti-MDA protein adducts antibody, Academic Bio-Medical Company, Inc. Houston, TX, USA), catalase (anti-catalase antibody, Calbiochem, Darmstadt, Germany), Mn-superoxide dismutase (SOD2, anti-SOD2 antibody, Santa Cruz Biotechnology, Santa Cruz, CA, USA), CuZn-superoxide dismutase (SOD1, anti-SOD1 antibody, Santa Cruz), b-cell lymphoma 2 (BCL-2, anti-BCL-2, antibody Santa Cruz), BCL-2 associated X protein (BAX, anti-BAX antibody, Santa Cruz), caspase-3 (anti-caspase3 antibody, Abcam, Cambridge, UK),

nucleoporin p62 (anti-p62 antibody, Sigma-Aldrich, St. Louis, MO, USA), beclin-1 (anti-beclin- 1 antibody, Santa Cruz), microtubule-associated protein 1 light-chain 3 (LC3B, anti-LC3B antibody, Cell Signaling, Massachusetts, USA), nuclear factor kappa-light-chain-enhancer of activated B cells (NF-kB) p65 (anti-NF-kB p65 antibody, Santa Cruz), sirtuin-1 (anti-sirtuin-1 antibody, EMD Millipore, Billerica, Massachusetts, USA) and glyceraldehyde-3-phosphate dehydrogenase (GAPDH, anti-GAPDH antibody, Santa Cruz) as the protein loading control to confirm identical protein loading among different lanes. Horseradish peroxidase (HRP)-conjugated secondary antibodies and a chemilumiscence kit (Thermo Scientific, Rockford, IL, USA) were used to detect the antigens from all samples.

PVDF membranes were scanned with the Molecular Imager Chemidoc XRS System (Bio–Rad Laboratories, Hercules, CA, USA) using the software Quantity One version 4.6.5 (Bio–Rad Laboratories) and optical densities of target proteins were quantified using the software Image Lab version 2.0.1 (Bio-Rad Laboratories). Final optical densities (arbitrary units) acquired in each group of mice corresponded to the average value of all the samples (lanes). Values of optical densities (arbitrary units) of cleaved caspase-3 were calculated as the ratio of cleaved protein (17kDa) to total caspase-3 protein content (34 kDa). Values of optical densities (arbitrary units) of LC3B-II/ LC3B-I were also calculated as the ratio of LC3B-II (14 kDa) to LC3B-I (16 kDa) protein content.

Standard stripping methodologies were employed to detect p62 protein levels in the same PVDF membranes of beclin-1. The loading control GAPDH was also detected using stripping methodologies in the study markers: protein tyrosine nitration, MDA-protein adducts, SOD1, SOD2, catalase, BAX, BCL-2, caspase-3, beclin-1, p62, LC3B, NF-kB p65, and Sirtuin-1. Briefly, primary and secondary antibodies were stripped off proteins using a stripping solution (25 nM glycine, pH 2.0, and 1% SDS) for 30 minutes. Membranes were subsequently washed two consecutive times (10 minutes each) with phosphate buffered saline and tween (PBST) at room temperature. Immediately afterwards, membranes were blocked with 1% BSA

and incubated with specific primary and secondary antibodies following the abovementioned procedures.

Statistical analysis

Using specific software (StudySize 2.0, CreoStat HB, Frolunda, Sweden) and assuming an alpha error of 0.05 and a minimum of 80% of standard power statistics, the sample size (N=9) was sufficiently great to identify a difference of 700 and 0.6 points in both tumor area and weight variables between groups, respectively. Shapiro-Wilk test was used to check the normality of the study variables. Therefore, data are expressed as mean and standard deviation in both tables and figures. Statistical Package for the Social Science (SPSS, version 22, SPSS Inc., Chicago, IL, USA) were used to compare the study variables between the two study groups using unpaired Student *T-test* and statistical significance was established at $p \leq 0.05$.

RESULTS

Monoclonal antibodies improve tumor burden and body weight in mice

As illustrated in Table 1 and Figure 2A, at the end day (30) of the study protocol, in the lung cancer mice compared to non-treated control mice, treatment with the cocktail of monoclonal antibodies significantly improved the following variables: final body weight, body weight gain with and without tumor, tumor weight (34% reduction), and tumor area (64% reduction). Importantly, levels of Ki-67 positive nuclei were significantly lower (27% reduction), while TUNEL positively stained nuclei were significantly higher (127% increased) in the tumors of mice treated with the monoclonal antibodies compared to those detected in the non-treated control animals (Figures 2B and 2C).

Table 1. Physiological and tumor characteristics in the study groups of mice.

Variables	Lung cancer mice	Lung cancer + monoclonal antibodies mice
Initial body weight (g)	20.41 (1.22)	20.34 (0.79)
Final body weight (g)	19.35 (2.25)	21.39 (1.57), *

Body weight gain (%)	-4.27 (10.47)	+5.16 (6.33), *
Body weight gain without tumor (%)	-15.06 (11.28)	-2.66 (8.35), *
Tumor weight (g)	2.38 (0.75)	1.57 (0.89), *

Variables are presented as mean (standard deviation).
Statistical significance: *: $p \leq 0.05$ between the two study groups of mice.

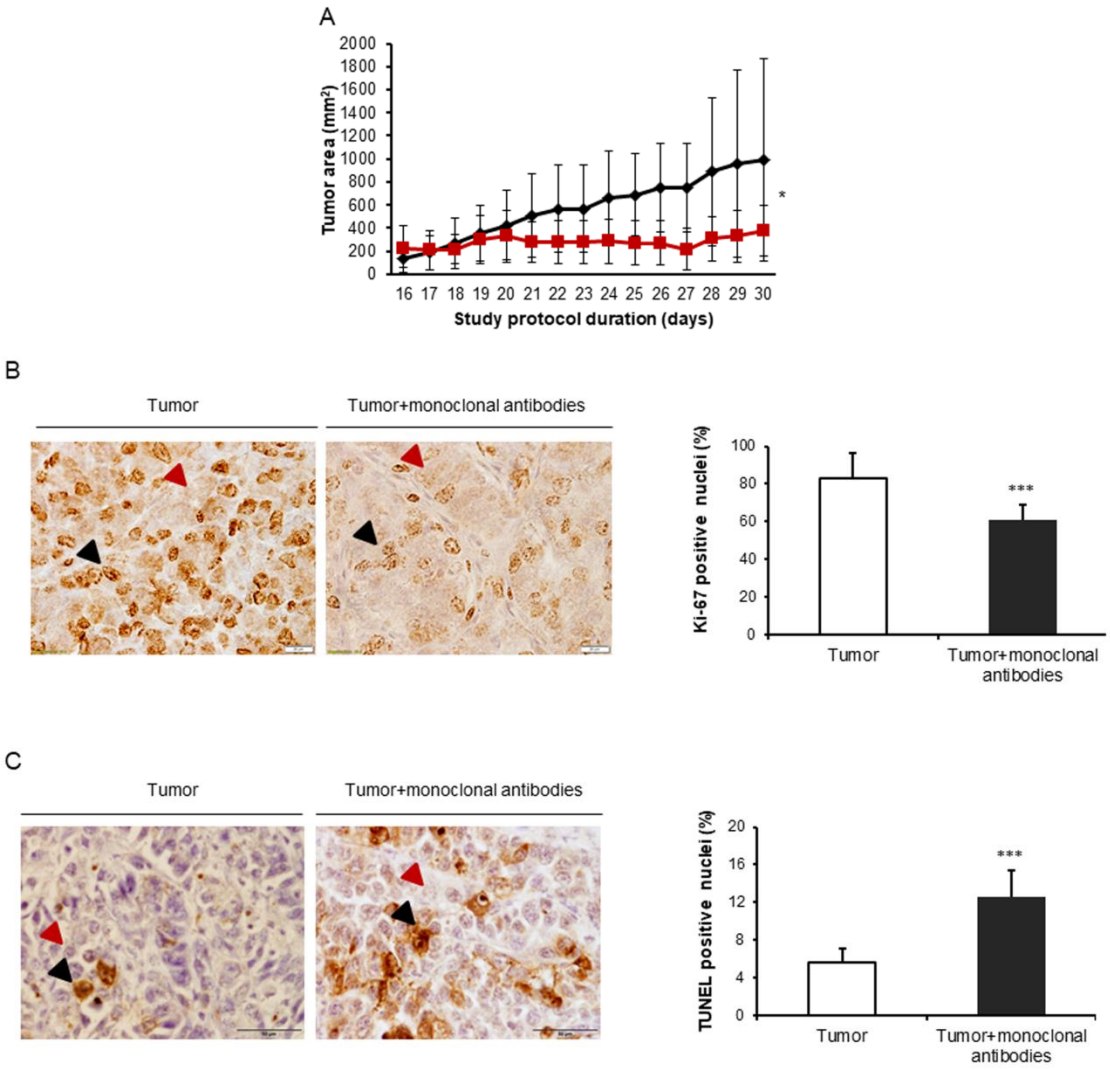

Figure 2: A) Mean values and standard deviation of subcutaneous tumor area (mm^2) of non-treated control lung cancer group of mice (black color) and lung cancer mice treated with monoclonal antibodies group (red color) during the study protocol. **B)** Representative histological sections (40x) and mean values and standard deviation of Ki-67 in the subcutaneous tumors of the non-treated control mice and the treated lung cancer animals. Black arrowheads point towards Ki-67 positively-stained nuclei (brown color), while red arrowheads point towards Ki-67 negatively-stained nuclei (purple color). **C)** Representative histological sections (40x) and mean values and standard deviation of TUNEL in the subcutaneous tumors of the non-treated control mice and the treated lung cancer animals. Black arrowheads point towards TUNEL positively-stained nuclei (brown color), while red arrowheads point towards TUNEL negatively-stained nuclei (purple color). Statistical significance: *: $p \leq 0.05$ and ***: $p \leq 0.001$ between lung cancer mice compared to lung cancer-monoclonal antibodies group.

Immune microenvironment in response to the immunomodulators

In tumors of mice treated with the monoclonal antibodies, the number of T cells (CD3, CD8 and CD4) was significantly greater than that observed in the non-treated mice (Table 2 and Figure 3). Levels of B cells (CD20), macrophages (CD68), and inflammatory cytokine (TNF-alpha) in the tumors did not show any significant difference between the two groups of mice (Table 2 and Figure 3).

Table 2. Immune microenvironment in the study groups of mice.

	Lung cancer mice	**Lung cancer + monoclonal antibodies mice**
T cells		
CD3+ cells (%)	8.34 (0.91)	11.30 (0.78), ***
CD4+ (cells/μm^2)	1.99×10^{-6} (0.44×10^{-6})	3.37×10^{-6} (1.49×10^{-6}), *
CD8+ cells (%)	5.16 (1.35)	7.86 (1.04), ***
B cells		
CD20+, Hscore 0 (%)	0.0 (0.0)	0.06 (0.82)
CD20+, Hscore 1 (%)	4.05 (4.41)	2.77 (2.12)
CD20+, Hscore 2 (%)	52.14 (14.29)	55.75 (5.15)
CD20+, Hscore 3 (%)	43.25 (18.12)	40.28 (4.64)
CD20+, Hscore 4 (%)	0.42 (0.47)	1.19 (0.60)
Macrophages		
CD68+ cells (%)	19.78 (6.50)	22.93 (7.63)
Inflammatory cytokines		
TNF-alpha +, Hscore 0 (%)	0.72 (1.49)	0.23 (0.39)
TNF-alpha +, Hscore 1 (%)	21.36 (12.84)	21.00 (13.46)
TNF-alpha +, Hscore 2 (%)	73.97 (13.11)	69.88 (7.40)
TNF-alpha +, Hscore 3 (%)	3.95 (2.97)	8.89 (12.04)

Values are expressed as mean (standard deviation).
Statistical significance: *$p \leq 0.05$ and ***$p \leq 0.001$ between the two experimental groups of mice.

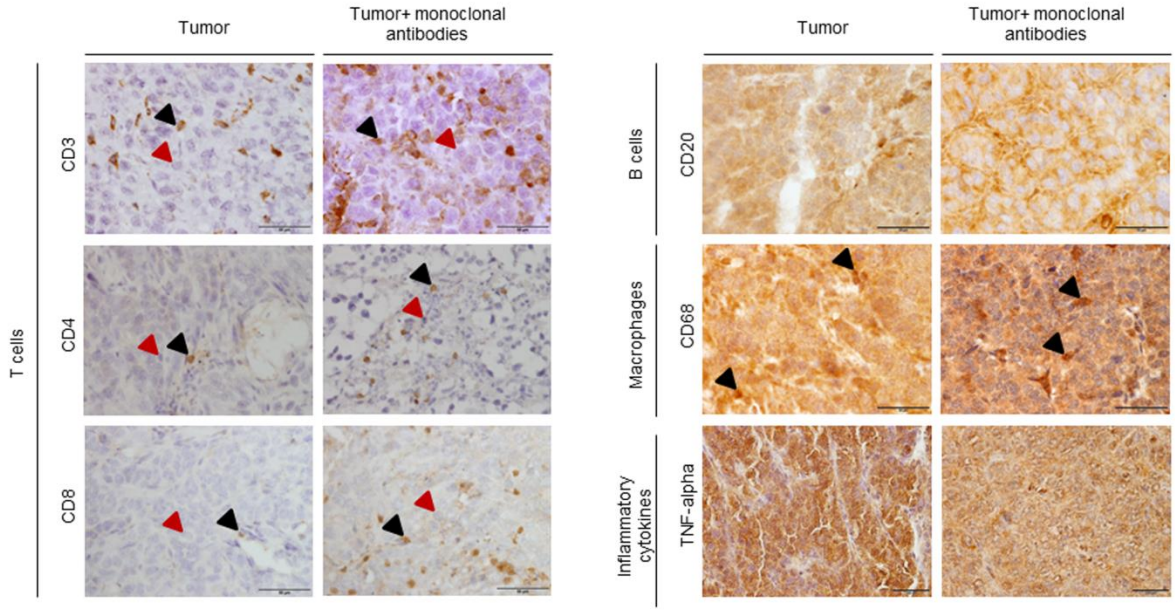

Figure 3: Representative examples of immunohistochemistry staining for CD3, CD8, CD4, CD20, CD68, and TNF-alpha in tumor samples of the different study groups of mice. All types of T cells (CD3, CD8 and CD4), B cells (CD20), macrophages (CD68) and inflammatory cytokines (TNF-alpha) are stained in brown color (black arrows), while negative nuclei are stained in purple color (red arrows).

Tumor oxidative stress in response to the immunomodulators

Compared to the non-treated mice, protein tyrosine nitration and oxidation (MDA-protein adducts) and cytosolic SOD1 levels were significantly greater in the tumors of the mice treated with the monoclonal antibodies, while no significant differences were detected in mitochondrial SOD2 or catalase protein levels between the two study groups (Figures 4A-4B and 5A-5C).

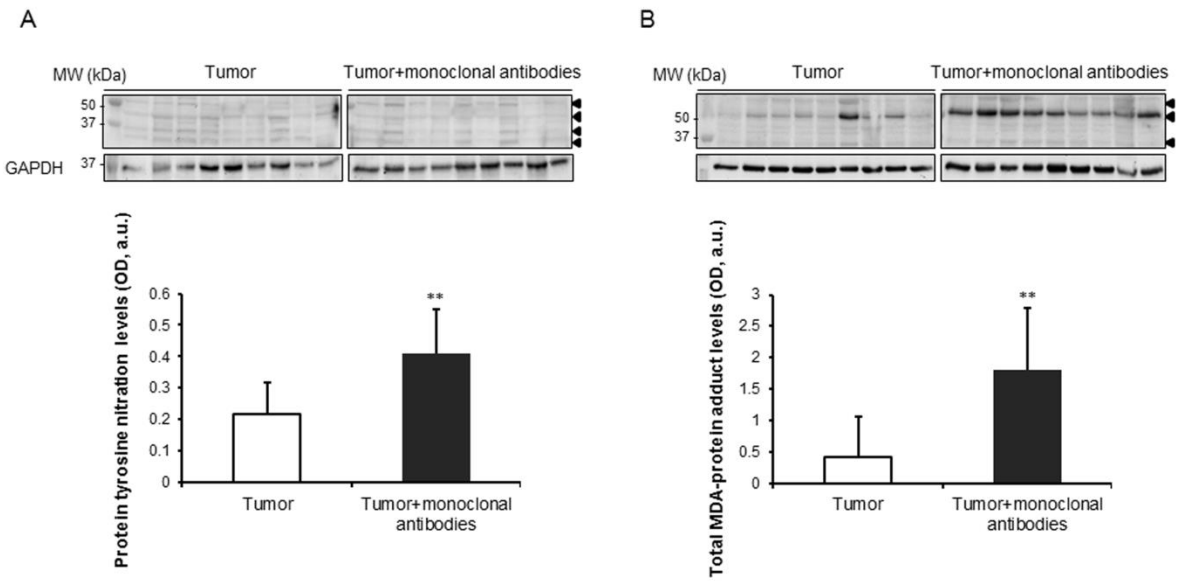

Figure 4: A) Representative immunoblots and mean values and standard deviation of total protein tyrosine nitration levels in subcutaneous tumors of lung cancer mice as measured by optical densities. **B)** Representative immunoblots and mean values and standard deviation of total MDA-protein adducts in subcutaneous tumors of lung cancer mice as measured by optical densities. Representative GAPDH is shown as the loading control. Statistical significance is represented as follows: **: $p \leq 0.01$ between non-treated controls (N=9) in white bars and treated lung cancer (N=9) mice in black bars. Definition of abbreviations: MDA, malondialdehyde; GAPDH, glyceraldehyde-3-phospate dehydrogenase; OD, optical densities; a.u., arbitrary units.

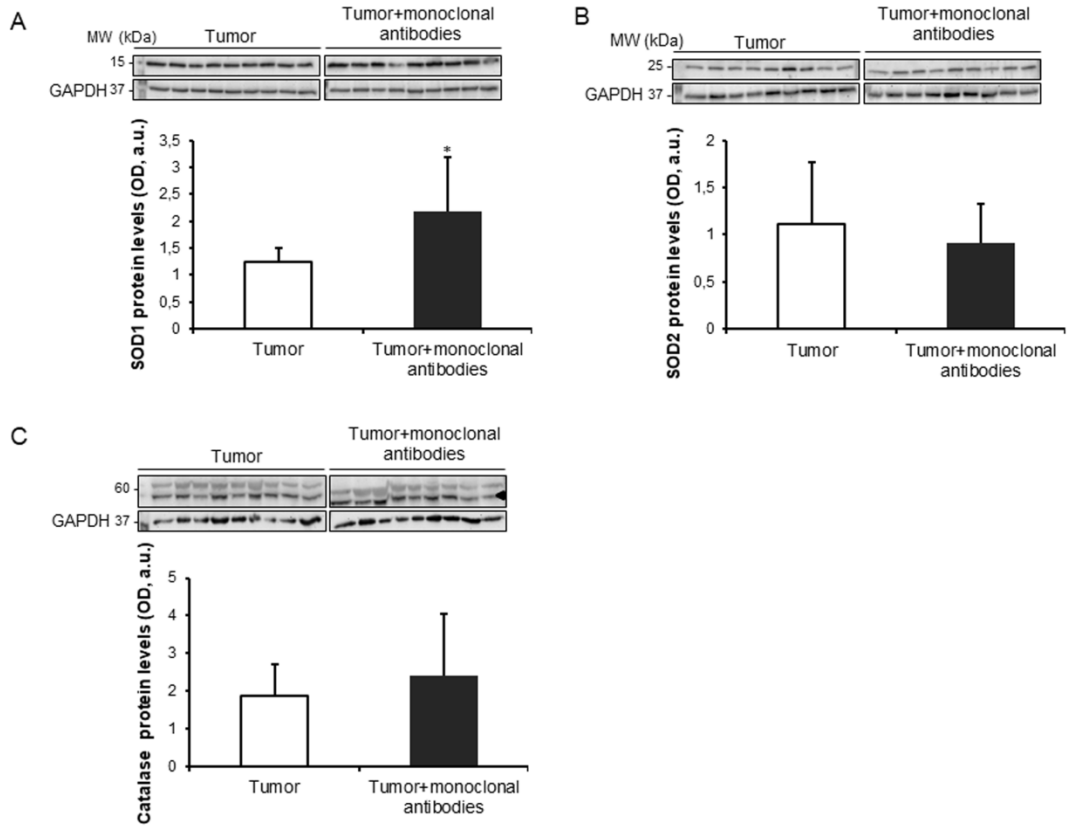

Figure 5: A) Representative immunoblots and mean values and standard deviation of SOD1 protein levels in subcutaneous tumors of lung cancer mice as measured by optical densities. **B)** Representative immunoblots and mean values and standard deviation of SOD2 protein levels in subcutaneous tumors of LC mice as measured by optical densities. **C)** Mean values and standard deviation of catalase protein levels in subcutaneous tumors of lung cancer mice as measured by optical densities. Representative GAPDH is shown as the loading control. Statistical significance is represented as follows: *: $p \leq 0.05$ between non-treated controls (N=9) in white bars and treated lung cancer (N=9) mice in black bars. Definition of abbreviations: SOD1, CuZn-superoxide dismutase; SOD2, Mn-superoxide dismutase; GAPDH, glyceraldehyde-3-phospate dehydrogenase; OD, optical densities; a.u., arbitrary units.

Tumor apoptosis and autophagy markers in response to immunomodulators

Treatment of the mice with the cocktail of monoclonal antibodies induced a significant rise in BCL-2 protein levels in the tumors compared to non-treated animals, while no significant differences were seen found in tumor BAX protein levels between the two study groups

(Figures 6A-6B). Cleaved caspase-3 protein levels significantly decreased in the tumors of mice treated with the monoclonal antibodies compared to the non-treated controls (Figure 6C). No significant differences were found in either beclin-1 or p62 tumor protein content between the two study groups, while treatment of the cancer animals with the monoclonal antibodies elicited a significant rise in the ratio of LC3-II to LC3-I in the tumors (Figures 7A-7C).

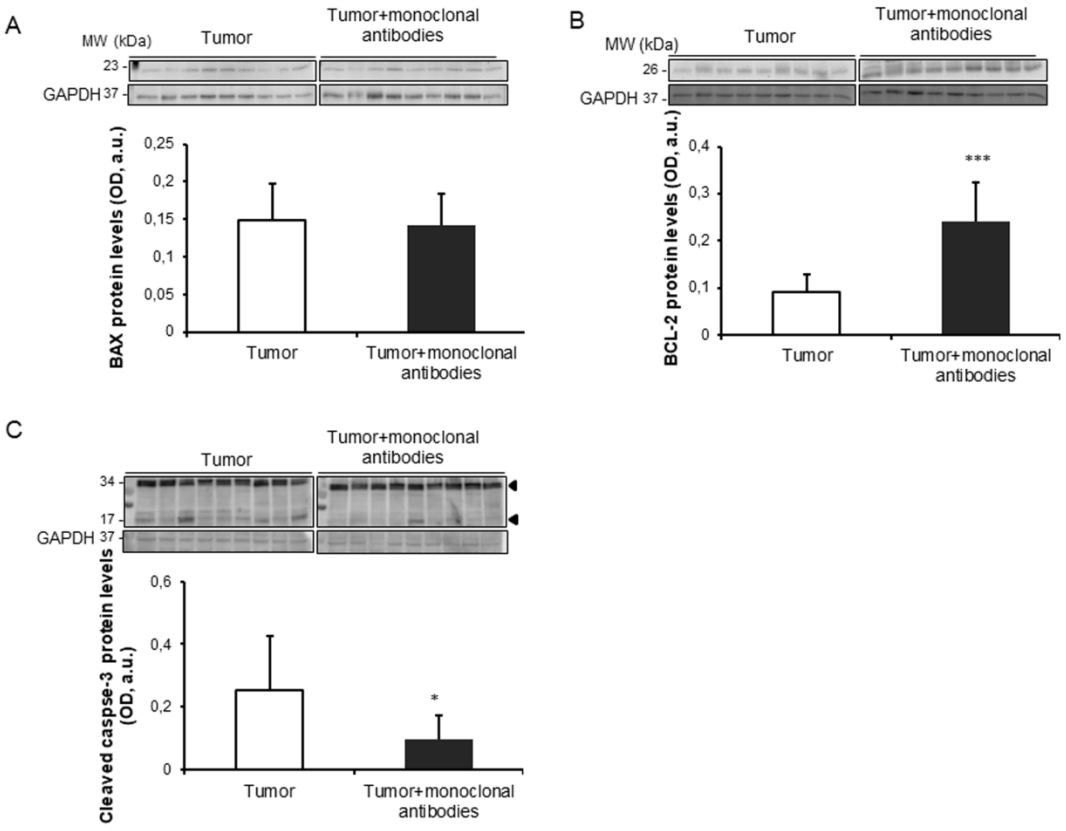

Figure 6: A) Representative immunoblots and mean values and standard deviation of BAX protein levels in subcutaneous tumors of lung cancer mice as measured by optical densities. **B)** Representative immunoblots and mean values and standard deviation of BCL-2 protein levels in subcutaneous tumors of LC mice as measured by optical densities. **C)** Representative immunoblots and mean values and standard deviation of activated caspase-3 protein levels in subcutaneous tumors of LC mice as measured by optical densities. Representative GAPDH is shown as the loading control. Statistical significance is represented as follows: *: $p \leq 0.05$ and ***: $p \leq 0.001$ between non-treated controls (N=9) in white bars and treated lung cancer (N=9) mice in black bars. Definition of abbreviations: BAX, BCL-2 associated X protein; BCL-2, b-cell lymphoma 2; GAPDH, glyceraldehyde-3-phospate dehydrogenase; OD, optical densities; a.u., arbitrary units.

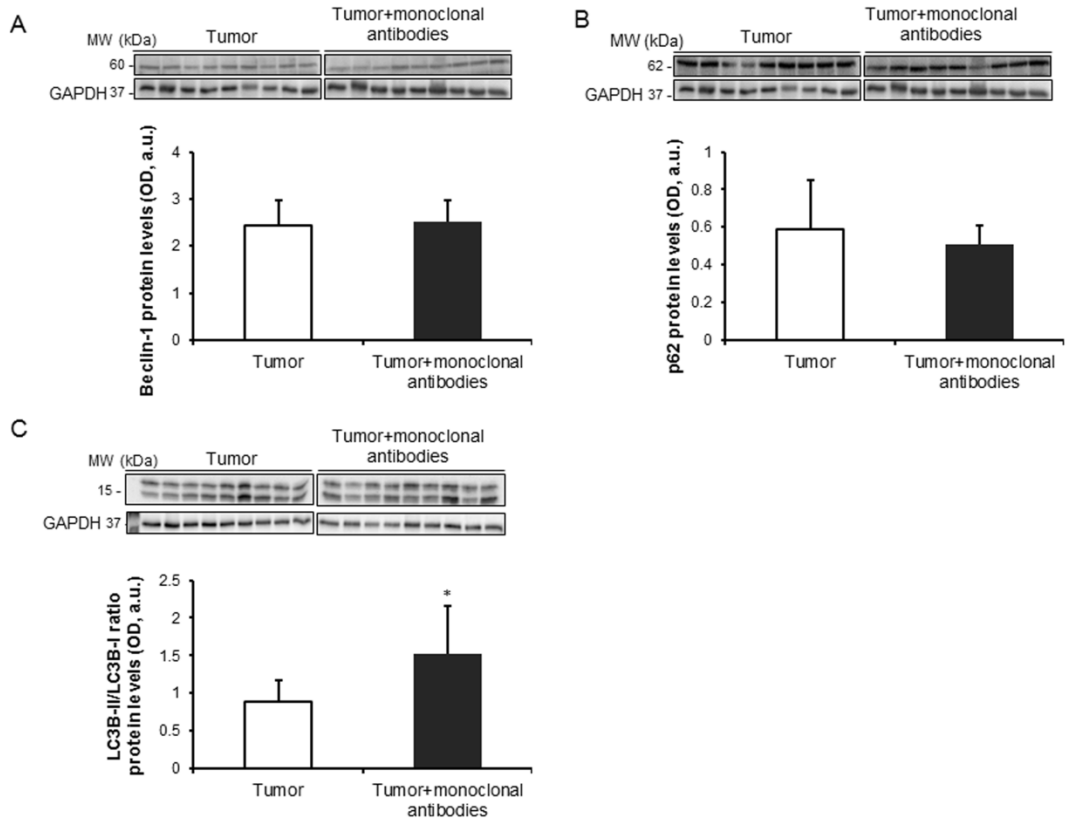

Figure 7: A) Representative immunoblots and mean values and standard deviation of Beclin-1 protein levels in subcutaneous tumors of LC mice as measured by optical densities. **B)** Representative immunoblots and mean values and standard deviation of p62 protein levels in subcutaneous tumors of LC mice as measured by optical densities. **C)** Representative immunoblots and mean values and standard deviation of total LC3-II/LC3-I protein in subcutaneous tumors of LC mice as measured by optical densities. Representative GAPDH is shown as the loading control. Statistical significance is represented as follows: *: $p \leq 0.05$ between non-treated controls (N=9) in white bars and treated lung cancer (N=9) mice in black bars. Definition of abbreviations: p62, nucleoporin p62; LC3, microtube-associated protein 1 light chain 3; GAPDH, glyceraldehyde-3-phospate dehydrogenase; OD, optical densities; a.u., arbitrary units.

Tumor signaling markers in response to immunomodulators

NF-kB p65 and the deacetylase sirtuin-1 protein levels were significantly higher in the tumors of the treated mice with the monoclonal antibodies compared to those seen in the non-treated animals (Figures 8A-8B).

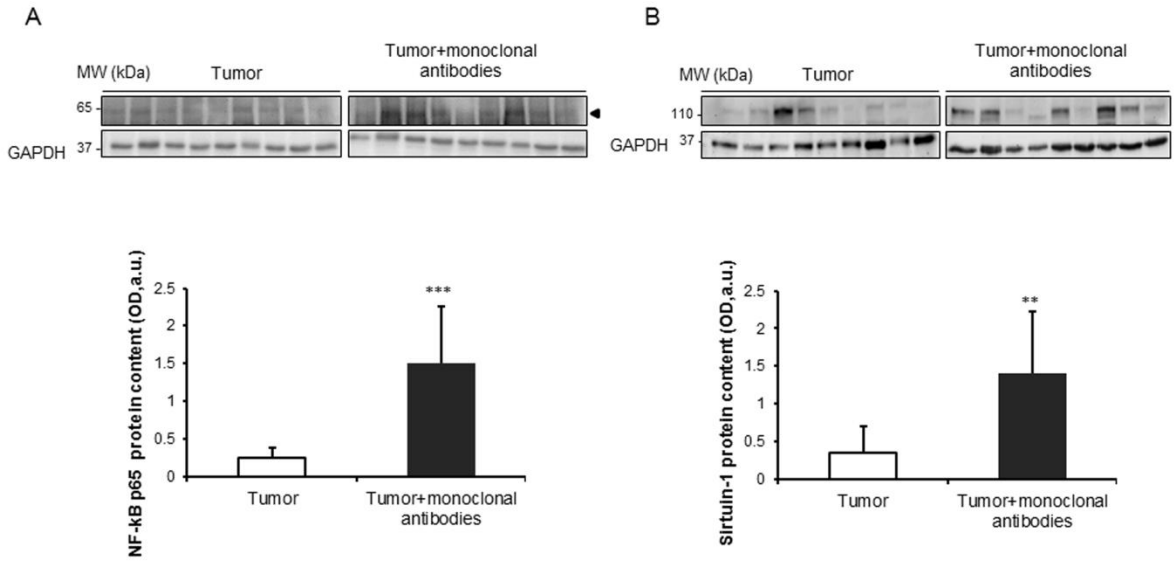

Figure 8: A) Representative immunoblots and mean values and standard deviation of NF-kB p65 protein levels in subcutaneous tumors of lung cancer mice as measured by optical densities. **B)** Representative immunoblots and mean values and standard deviation of sirtuin-1 protein levels in subcutaneous tumors of lung cancer mice as measured by optical densities. Representative GAPDH is shown as the loading control. Statistical significance is represented as follows: and **: $p \leq 0.01$ and ***: $p \leq 0.001$ between non-treated controls (N=9) in white bars and treated lung cancer (N=9) mice in black bars. Definition of abbreviations: NF-kB, nuclear factor kappa-light-chain-enhancer of activated B cells; GAPDH, glyceraldehyde-3-phospate dehydrogenase; OD, optical densities; a.u., arbitrary units.

DISCUSSION

In the present study, treatment of the tumor-bearing mice with a cocktail of monoclonal antibodies that specifically targeted immune check-points and pathways elicited a significant reduction of tumor proliferation rates and sizes through the induction of several biological mechanisms that are discussed below. Thus, the study hypothesis has been confirmed to a great extent.

In the tumors of the mice treated with the cocktail of monoclonal antibodies, the area was significantly reduced at the end of the study period. These are relevant findings that confirm the efficacy of the treatment with the immunomodulators of the tumor cells in the mice. These results are in line with those previously reported, in which a complete regression of the tumors (melanoma and lung cancer) was attained following intratumoral treatment of the mice with the same cocktail of monoclonal antibodies [18;19]. Importantly, numbers of T cell subtypes

significantly increased in the tumors of the mice that received treatment with the checkpoint inhibitors in the present study. Importantly, the immunomodulators were injected intraperitoneally with the aim to mimic the treatments applied in patients, in whom drugs are usually administered systemically. In this investigation, a complete regression of the tumors was not achieved probably as a result of the systemic administration of the drugs compared to previous reports [18;19]. Nonetheless, in the tumor-bearing mice that received the medical treatment with the immunomodulators a significant reduction in tumor burden as measured by both tumor weight (34%) and area (64 %) was observed.

Interestingly, the number of tumor proliferating cells was also significantly lower in the tumors of the mice treated with the monoclonal antibodies than in the non-treated tumor-bearing rodents. These results suggest that cell cycle arrest probably due to alterations in cyclin expression levels may account for the reduced levels of Ki-67-positively stained nuclei encountered in the adenocarcinoma cells of the treated tumor-bearing mice. Moreover, these findings are also in agreement with previous investigations, in which expression levels of Ki-67 were significantly reduced (34%) in the tumors of mice treated with several selective inhibitors of cell survival pathways [12], in those from transgenic mice deficient for either poly(ADP-ribose) polymerases (PARP)-1 and -2 enzymes [26], and in those of rodents treated with pharmacological inhibitors of PARP activity [41]. Taken together, these results are also very consistent with the above-mentioned reduced tumor area and weight seen in the tumor-bearing mice treated with the immunomodulators at the end of the study period.

Oxidative stress was assessed using several indirect markers in the tumor cells of both groups of mice. Importantly, protein levels of protein tyrosine nitration and total MDA-protein adducts were significantly greater in the tumor cells of the mice that received treatment with the monoclonal antibodies. These results are in agreement with those previously observed in another investigation in which protein oxidation levels were also increased in the tumors of Parp-1$^{-/-}$ and Parp-2$^{-/-}$ mice [26]. In the present investigation, levels of the antioxidant enzyme

SOD1, but not those of SOD2 or catalase, were significantly greater in the tumors of the lung cancer-bearing mice treated with the monoclonal antibodies. These results are in line with those encountered in the tumors of mice treated with the proteasome inhibitor bortezomib [12]. The rise in the expression of cytosolic SOD1 levels may have been a response to counterbalance the deleterious effects of increased oxidative stress in the tumor cells as previously suggested [12]. Altogether, a rise in several oxidative stress markers was observed in the tumors of the mice treated with the cocktail of monoclonal antibodies. These findings may imply that in response to treatment with the immunomodulators, oxidative stress may drive cell cycle arrest and tumor cell death independently of the immune response [42].

Oxidative stress may also trigger several important cellular pathways such as cell death, apoptosis, and autophagy. For instance, in the tumor cells of the mice treated with the immmunomodulators, levels of TUNEL-positive nuclei were significantly greater. These results are consistent with those previously reported, in which different therapeutic strategies also elicited a rise in apoptotic markers [12;26]. The increase in apoptotic markers of cancer cells was also demonstrated in previous investigations in which the animals were treated with inhibitors of PARP [41;43-45].

A rise in the autophagy marker LC3B was observed in the tumor cells of the mice treated with the immunomodulators compared to non-treated control rodents. These results imply that autophagy may also mediate the reduced tumor burden observed in the mice that received treatment with the cocktail of monoclonal antibodies. In fact, similar results were previously demonstrated in the tumors of mice that were genetically deficient for either PARP-1 or PARP-2 proteins, especially the latter [26].

The deacetylase sirtuin-1 may play a role in autophagy as a result of its upstream regulation of LC3B [46]. In the current study, a significant rise in protein levels of sirtuin-1 was detected in the tumor cells of the mice treated with the monoclonal antibodies compared to non-treated animals. On the other hand, sirtuin-1 may also play a role in the regulation of tumor

microenvironment of the immune cells [47]. These results imply that sirtuin-1 probably interfered with immune cells [47], leading to changes in the tumor microenvironment (from Th2 type to Th1 immunity) as previously demonstrated [18;19], which may further contribute to the observed reduced tumor burden in the mice treated with the monoclonal antibodies. Despite the relevance of this question, it will have to be fully elucidated in future investigations as it was clearly beyond the objectives of the current investigation.

Conclusions

We have demonstrated that immunomodulators with different mechanisms of action elicited a reduction in tumor burden as measured by tumor size and weight through several biological mechanisms, namely decreased tumor proliferation rates and increased T cell counts, oxidative stress, apoptosis, autophagy, and sirtuin-1 levels, which may have interfered with the immune profile of the tumor microenvironment. Future research should be devoted to the elucidation of the specific contribution of each mechanism (reduced tumor proliferation, increased tumor degradation, and stimulation of the immune tumor microenvironment) to the reduced tumor burden seen in this animal model of lung cancer. These findings may have potential therapeutic implications in patients under treatment with immunomodulators for their lung neoplasms.

ACKNOWLEDGEMENTS

The authors are also very grateful to Xavier Duran for his contribution to the statistical analyses of the study results and to Dr. Salazar-Degracia for her help with part of the animal experiments. This study has been supported by CIBERES; FIS 14/00713 (FEDER); FIS 18/00075 (FEDER); SEPAR 2016; SEPAR 2018; FUCAP 2016; Unrestricted grant from Menarini SA 2018 (Spain), *and GlaxoSmithKline SA* (Spain) 2018.

All authors have read the Journal's policy on disclosure of potential conflicts of interest.

Disclosure of potential conflicts of interest by the authors: None to disclose.

Editorial support: None to declare.

Reference List

1 Siegel RL, Miller KD, Jemal A: Cancer statistics, 2018. CA Cancer J Clin 2018;68:7-30.

2 Alvarez FV, Trueba IM, Sanchis JB, Lopez-Rodo LM, Rodriguez Suarez PM, de Cos Escuin JS, Barreiro E, Henar Borrego PM, Vicente CD, Aldeyturriaga JF, Gamez GP, Garrido LP, Leon AP, Izquierdo Elena JM, Novoa Valentin NM, Rivas de Andres JJ, Crespo IR, Velazquez AS, Seijo Maceiras LM, Reina SS, Bujanda DA, Avila Martinez RJ, de Granda Orive JI, Martinez EH, Gude VD, Flor RE, Freixinet Gilart JL, Garcia Jimenez MD, Alarza FH, Sarmiento SH, Honguero Martinez AF, Jimenez Ruiz CA, Sanz IL, Mariscal de AA, Martinez VP, Menal MP, Perez LM, Olmedo Garcia ME, Rombola CA, Arregui IS, Somiedo GM, V, Trivino Ramirez AI, Trujillo Reyes JC, Vallejo C, Lozano PV, Simo GV, Zulueta JJ: Recommendations of the Spanish Society of Pneumology and Thoracic Surgery on the diagnosis and treatment of non-small-cell lung cancer. Arch Bronconeumol 2016;52 Suppl 1:2-62.

3 Malvezzi M, Carioli G, Bertuccio P, Boffetta P, Levi F, La VC, Negri E: European cancer mortality predictions for the year 2017, with focus on lung cancer. Ann Oncol 2017;28:1117-1123.

4 Miravitlles M, Soler-Cataluna JJ, Calle M, Molina J, Almagro P, Quintano JA, Trigueros JA, Cosio BG, Casanova C, Antonio RJ, Simonet P, Rigau D, Soriano JB, Ancochea J: Spanish Guidelines for Management of Chronic Obstructive Pulmonary Disease (GesEPOC) 2017. Pharmacological Treatment of Stable Phase. Arch Bronconeumol 2017;53:324-335.

5 Vogelmeier CF, Criner GJ, Martinez FJ, Anzueto A, Barnes PJ, Bourbeau J, Celli BR, Chen R, Decramer M, Fabbri LM, Frith P, Halpin DM, Lopez Varela MV, Nishimura M, Roche N, Rodriguez-Roisin R, Sin DD, Singh D, Stockley R, Vestbo J, Wedzicha JA, Agusti A: Global Strategy for the Diagnosis, Management, and Prevention of Chronic Obstructive Lung Disease 2017 Report: GOLD Executive Summary. Arch Bronconeumol 2017;53:128-149.

6 Villar AF, Muguruza T, I, Belda SJ, Molins Lopez-Rodo L, Rodriguez Suarez PM, Sanchez de Cos EJ, Barreiro E, Borrego Pintado MH, Disdier VC, Flandes AJ, Gamez GP, Garrido LP, Leon AP, Izquierdo Elena JM, Novoa Valentin NM, Rivas de Andres JJ, Royo C, I, Salvatierra VA, Seijo Maceiras LM, Solano RS, Aguiar BD, Avila Martinez RJ, de Granda Orive JI, de Higes ME, Diaz-Hellin G, V, Embun FR, Freixinet Gilart JL, Garcia Jimenez MD, Hermoso AF, Hernandez SS, Honguero Martinez AF, Jimenez Ruiz CA, Lopez S, I, Mariscal de AA, Martinez VP, Menal MP, Mezquita PL, Olmedo Garcia ME, Rombola CA, San MA, I, de Valle Somiedo GM, Trivino Ramirez AI, Trujillo Reyes JC, Vallejo C, Vaquero LP, Varela SG, Zulueta JJ: Executive summary of the SEPAR recommendations for the diagnosis and treatment of non-small cell lung cancer. Arch Bronconeumol 2016;52:378-388.

7 Conway EM, Pikor LA, Kung SH, Hamilton MJ, Lam S, Lam WL, Bennewith KL: Macrophages, Inflammation, and Lung Cancer. Am J Respir Crit Care Med 2016;193:116-130.

8 Mateu-Jimenez M, Curull V, Pijuan L, Sanchez-Font A, Rivera-Ramos H, Rodriguez-Fuster A, Aguilo R, Gea J, Barreiro E: Systemic and Tumor Th1 and Th2 Inflammatory Profile and Macrophages in Lung Cancer: Influence of Underlying Chronic Respiratory Disease. J Thorac Oncol 2017;12:235-248.

9 O'Byrne KJ, Dalgleish AG: Chronic immune activation and inflammation as the cause of malignancy. Br J Cancer 2001;85:473-483.

10 O'Callaghan DS, O'Donnell D, O'Connell F, O'Byrne KJ: The role of inflammation in the pathogenesis of non-small cell lung cancer. J Thorac Oncol 2010;5:2024-2036.

11 Barreiro E, Fermoselle C, Mateu-Jimenez M, Sanchez-Font A, Pijuan L, Gea J, Curull V: Oxidative stress and inflammation in the normal airways and blood of patients with lung cancer and COPD. Free Radic Biol Med 2013;65:859-871.

12 Mateu-Jimenez M, Fermoselle C, Rojo F, Mateu J, Pena R, Urtreger AJ, Diament MJ, Joffe ED, Pijuan L, Herreros AG, Barreiro E: Pharmacological Approaches in an Experimental Model of Non-Small Cell Lung Cancer: Effects on Tumor Biology. Curr Pharm Des 2016;22:5300-5310.

13 Mateu-Jimenez M, Sanchez-Font A, Rodriguez-Fuster A, Aguilo R, Pijuan L, Fermoselle C, Gea J, Curull V, Barreiro E: REDOX IMBALANCE IN LUNG CANCER OF PATIENTS WITH UNDERLYING CHRONIC RESPIRATORY CONDITIONS. Mol Med 2016.

14 Barreiro E, Bustamante V, Curull V, Gea J, Lopez-Campos JL, Munoz X: Relationships between chronic obstructive pulmonary disease and lung cancer: biological insights. J Thorac Dis 2016;8:E1122-E1135.

15 Pore MM, Hiltermann TJ, Kruyt FA: Targeting apoptosis pathways in lung cancer. Cancer Lett 2013;332:359-368.

16 Mateu-Jimenez M, Curull V, Rodriguez-Fuster A, Aguilo R, Sanchez-Font A, Pijuan L, Gea J, Barreiro E: Profile of epigenetic mechanisms in lung tumors of patients with underlying chronic respiratory conditions. Clin Epigenetics 2018;10:7.

17 Schreiber RD, Old LJ, Smyth MJ: Cancer immunoediting: integrating immunity's roles in cancer suppression and promotion. Science 2011;331:1565-1570.

18 Dai M, Wei H, Yip YY, Feng Q, He K, Popov V, Hellstrom I, Hellstrom KE: Long-lasting complete regression of established mouse tumors by counteracting Th2 inflammation. J Immunother 2013;36:248-257.

19 Dai M, Yip YY, Hellstrom I, Hellstrom KE: Curing mice with large tumors by locally delivering combinations of immunomodulatory antibodies. Clin Cancer Res 2015;21:1127-1138.

20 Tsou P, Katayama H, Ostrin EJ, Hanash SM: The Emerging Role of B Cells in Tumor Immunity. Cancer Res 2016;76:5597-5601.

21 Yonezawa A, Dutt S, Chester C, Kim J, Kohrt HE: Boosting Cancer Immunotherapy with Anti-CD137 Antibody Therapy. Clin Cancer Res 2015;21:3113-3120.

22 Chen DS, Mellman I: Elements of cancer immunity and the cancer-immune set point. Nature 2017;541:321-330.

23 Blank CU, Enk A: Therapeutic use of anti-CTLA-4 antibodies. Int Immunol 2015;27:3-10.

24 Haanen JB, Robert C: Immune Checkpoint Inhibitors. Prog Tumor Res 2015;42:55-66.

25 Rolfo C, Caglevic C, Santarpia M, Araujo A, Giovannetti E, Gallardo CD, Pauwels P, Mahave M: Immunotherapy in NSCLC: A Promising and Revolutionary Weapon. Adv Exp Med Biol 2017;995:97-125.

26 Mateu-Jimenez M, Cucarull-Martinez B, Yelamos J, Barreiro E: Reduced tumor burden through increased oxidative stress in lung adenocarcinoma cells of PARP-1 and PARP-2 knockout mice. Biochimie 2016;121:278-286.

27 Chacon-Cabrera A, Fermoselle C, Urtreger AJ, Mateu-Jimenez M, Diament MJ, de Kier Joffe ED, Sandri M, Barreiro E: Pharmacological strategies in lung cancer-induced cachexia: effects on muscle proteolysis, autophagy, structure, and weakness. J Cell Physiol 2014;229:1660-1672.

28 Chacon-Cabrera A, Fermoselle C, Salmela I, Yelamos J, Barreiro E: MicroRNA expression and protein acetylation pattern in respiratory and limb muscles of Parp-1(-/-) and Parp-2(-/-) mice with lung cancer cachexia. Biochim Biophys Acta 2015;1850:2530-2543.

29 Chacon-Cabrera A, Mateu-Jimenez M, Langohr K, Fermoselle C, Garcia-Arumi E, Andreu AL, Yelamos J, Barreiro E: Role of Parp Activity in Lung Cancer-induced Cachexia: Effects on Muscle Oxidative Stress, Proteolysis, Anabolic Markers and Phenotype. J Cell Physiol 2017.

30 Diament MJ, Garcia C, Stillitani I, Saavedra VM, Manzur T, Vauthay L, Klein S: Spontaneous murine lung adenocarcinoma (P07): A new experimental model to study paraneoplastic syndromes of lung cancer. Int J Mol Med 1998;2:45-50.

31 Diament MJ, Peluffo GD, Stillitani I, Cerchietti LC, Navigante A, Ranuncolo SM, Klein SM: Inhibition of tumor progression and paraneoplastic syndrome development in a murine lung adenocarcinoma by medroxyprogesterone acetate and indomethacin. Cancer Invest 2006;24:126-131.

32 Urtreger AJ, Diament MJ, Ranuncolo SM, Del C, V, Puricelli LI, Klein SM, de Kier Joffe ED: New murine cell line derived from a spontaneous lung tumor induces paraneoplastic syndromes. Int J Oncol 2001;18:639-647.

33 Chen DS, Mellman I: Oncology meets immunology: the cancer-immunity cycle. Immunity 2013;39:1-10.

34 Forsthuber TG, Cimbora DM, Ratchford JN, Katz E, Stuve O: B cell-based therapies in CNS autoimmunity: differentiating CD19 and CD20 as therapeutic targets. Ther Adv Neurol Disord 2018;11:1756286418761697.

35 Jin HT, Ahmed R, Okazaki T: Role of PD-1 in regulating T-cell immunity. Curr Top Microbiol Immunol 2011;350:17-37.

36 Selby MJ, Engelhardt JJ, Quigley M, Henning KA, Chen T, Srinivasan M, Korman AJ: Anti-CTLA-4 antibodies of IgG2a isotype enhance antitumor activity through reduction of intratumoral regulatory T cells. Cancer Immunol Res 2013;1:32-42.

37 Chacon-Cabrera A, Gea J, Barreiro E: Short- and Long-Term Hindlimb Immobilization and Reloading: Profile of Epigenetic Events in Gastrocnemius. J Cell Physiol 2016.

38 Salazar-Degracia A, Granado-Martinez P, Millan-Sanchez A, Tang J, Pons-Carreto A, Barreiro E: Reduced lung cancer burden by selective immunomodulators elicits improvements in muscle proteolysis and strength in cachectic mice. J Cell Physiol 2019.

39 Mateu-Jimenez M, Fermoselle C, Rojo F, Mateu J, Pena R, Urtreger AJ, Diament MJ, Joffe ED, Pijuan L, Herreros AG, Barreiro E: Pharmacological Approaches in an Experimental Model of Non-Small Cell Lung Cancer: Effects on Tumor Biology. Curr Pharm Des 2016;22:5300-5310.

40 Millares L, Barreiro E, Cortes R, Martinez-Romero A, Balcells C, Cascante M, Enguita AB, Alvarez C, Rami-Porta R, Sanchez de CJ, Seijo L, Monso E: Tumor-associated metabolic and inflammatory responses in early stage non-small cell lung cancer: Local patterns and prognostic significance. Lung Cancer 2018;122:124-130.

41 Albert JM, Cao C, Kim KW, Willey CD, Geng L, Xiao D, Wang H, Sandler A, Johnson DH, Colevas AD, Low J, Rothenberg ML, Lu B: Inhibition of poly(ADP-ribose) polymerase enhances cell death and improves tumor growth delay in irradiated lung cancer models. Clin Cancer Res 2007;13:3033-3042.

42 Su X, Jiang X, Meng L, Dong X, Shen Y, Xin Y: Anticancer Activity of Sulforaphane: The Epigenetic Mechanisms and the Nrf2 Signaling Pathway. Oxid Med Cell Longev 2018;2018:5438179.

43 Gangopadhyay NN, Luketich JD, Opest A, Visus C, Meyer EM, Landreneau R, Schuchert MJ: Inhibition of poly(ADP-ribose) polymerase (PARP) induces apoptosis in lung cancer cell lines. Cancer Invest 2011;29:608-616.

44 Gaymes TJ, Shall S, MacPherson LJ, Twine NA, Lea NC, Farzaneh F, Mufti GJ: Inhibitors of poly ADP-ribose polymerase (PARP) induce apoptosis of myeloid leukemic cells: potential for therapy of myeloid leukemia and myelodysplastic syndromes. Haematologica 2009;94:638-646.

45 Karpel-Massler G, Pareja F, Aime P, Shu C, Chau L, Westhoff MA, Halatsch ME, Crary JF, Canoll P, Siegelin MD: PARP inhibition restores extrinsic apoptotic sensitivity in glioblastoma. PLoS One 2014;9:e114583.

46 Huang R, Xu Y, Wan W, Shou X, Qian J, You Z, Liu B, Chang C, Zhou T, Lippincott-Schwartz J, Liu W: Deacetylation of nuclear LC3 drives autophagy initiation under starvation. Mol Cell 2015;57:456-466.

47 Arts RJW, Huang PK, Yang, Joosten LAB, van der Meer JWM, Oppenheim JJ, Netea MG, Cheng SC: High-Mobility Group Nucleosome-Binding Protein 1 as Endogenous Ligand Induces Innate Immune Tolerance in a TLR4-Sirtuin-1 Dependent Manner in Human Blood Peripheral Mononuclear Cells. Front Immunol 2018;9:526.